Robust Predictive Current Control of Induction Motors Based on Linear Extended State Observer

Yongchang Zhang[1, 2*], *Xing Wang*[1], *Haitao Yang*[1], *Boyue Zhang*[1] *and Jose Rodriguez*[3]

(1. Inverter Technologies Engineering Research Center of Beijing,
North China University of Technology, Beijing 100144, China;
2. School of Electrical and Electroric Engineering, North China Electric Power University,
Beijing 102206, China;
3. College of Engineering, Universidad Andres Bello, Santiago 8370146, Chile)

Abstract: Model predictive current control can achieve fast dynamic response and satisfactory steady-state performance for induction motor (IM) drives. However, many motor parameters are required to implement the control algorithm. Consequently, if the motor parameters used in the controller are not accurate, the performance may deteriorate. In this paper, a new robust predictive current control is proposed to improve robustness against parameter mismatches. The proposed method employs an ultra-local model to replace the mathematical model of the IM. Additionally, to improve the control performance, a linear extended state observer is developed for disturbance estimation. Experimental tests confirm that satisfactory tracking performance can still be obtained although the motor parameters may not be accurately set in the controller.

Keywords: Induction motor drives, current control, predictive control, observers, robustness

1 Introduction

Induction motors (IMs) are widely used in industrial fields due to their advantages, such as simple structure, high reliability, easy maintenance, and ability to adapt to various complex environments. At present, the high-performance control algorithms for IMs used in industrial fields include field-oriented control (FOC) [1] and direct torque control (DTC) [2]. The FOC can achieve acceptable steady-state performance, but proper proportional-integral parameters should be designed. The DTC can achieve fast dynamic performance with a simple structure; however, classic switching table-based DTC presents relatively high torque ripples [3]. In recent years, model predictive control (MPC) [4-5] has received increasing attention owing to its simple principle, fast transient response, and flexibility in handling nonlinear constraints and multiple variable control [6-7].

Many researchers have studied MPC and proposed new methods to improve its performance or reduce the control complexity. In Ref. [8], a model predictive flux control is proposed to eliminate weighting, and the amount of calculations is significantly reduced. In Ref. [9], the design of the weighting factor for stator flux is optimized to reduce torque ripples. Although the MPC exhibits satisfactory steady-state performance and fast dynamic response, it is highly dependent on the precision of motor parameters because these are required for predicting the evolution of the control variable.

In practical application, the motor parameters can change under different working conditions. For example, the stator and rotor resistances can change with temperature variations [10]. When the motor parameters used in the predictive controller do not conform with their actual values, the derived voltage vector may not be the optimal; consequently, the overall control performance deteriorates. To resolve these problems, several methods for increasing robustness have been investigated in the existing literature, including online parameter adaption [11], disturbance observer [12], extended state observer (ESO) [13]

Manuscript received August 18, 2020; revised November 12, 2020; accepted December 20, 2020. Date of publication March 31, 2021; date of current version March 10, 2021.
* Corresponding Author, E-mail: zyc@ncepu.edu.cn
Digital Object Identifier: 10.23919/CJEE.2021.000009

and model-free control (MFC) [14].

An online adaption method can be applied to track the actual model parameters. In Ref. [15], an online parameter estimation scheme based on a discrete-time dynamic model was developed to estimate the stator inductance, stator resistance, rotor flux linkage, and load torque. In Ref. [16], an online identification method based on a reference model, which estimates the motor parameters by nullifying the current estimation error, is presented. Compared with online identification based on Kalman filter, this method improves convergence dynamics and overall system stability. However, during steady state, the simultaneous estimation of multiple model parameters based on the fundamental motor model is infeasible [16].

The disturbance observer and ESO have also received considerable attention in the field of motor control. These methods can improve the robustness of the control system by observing and compensating for the lumped disturbance. In Ref. [13], a disturbance observer is investigated for the predictive torque control of IM drives subject to load disturbance, parameter errors, and digital delay. In Ref. [17], a robust speed and flux estimation is developed to reduce the impact of external disturbance and internal estimation error. Using the observer-based method, the motor can still maintain satisfactory control performance despite motor parameter variations and external disturbances. However, most of the above techniques are developed based on the machine mathematical model, and motor parameters are still required [18].

Recently, various MFC schemes have been introduced to improve parameter robustness for motor drives. Lin et al. [19] proposed a model-free predictive current control (MFPCC) based on the information of the previous current difference. Although this method does not require any motor parameters, it necessitates current sampling twice in one control period. Therefore, proper timing to trigger analog-to-digital conversion for current measurement is necessary to avoid the switching harmonics, which can increase implementation complexity in the sampled current. Fliess et al. [20] combined the principles of MFC and intelligent proportional-integral-derivative controllers. The method exhibits satisfactory robustness against unknown disturbances and parameter mismatches. The basic idea of this strategy is that the system is defined as an ultra-local model, which is estimated using differential algebra. In Ref. [14], an ultra-local model-based model-free current control (MFCC), which only relies on the input and output data of the controlled system and achieves satisfactory control performance for a surface-mounted permanent-magnet synchronous machine drive, is proposed. However, up to five parameters require tuning.

In this paper, a new robust predictive current control (RPCC) method based on the ultra-local model and a linear extended state observer (LESO) is investigated for IM drives. The work contribution can be highlighted by the following points.

(1) In the proposed strategy, the unknown part in the ultra-local model is estimated using the LESO. Compared with the conventional MFCC, the proposed RPCC reduces the amount of calculations. Further, it only uses two control parameters, thus simplifying the tuning effort.

(2) In existing literature, observers are used to estimate the influence of mismatched parameters based on the mathematical motor model. These methods still require knowing the motor parameters. The proposed method introduces an ultra-local model; it can estimate the total unknown part of the system without the motor model. Hence, applying the control scheme to other motors is convenient.

The effectiveness of the proposed RPCC is validated by experimental tests performed on a 2.2 kW IM drive.

2 IM drive system model

The voltage and flux equations of IM described by space vectors in a stationary frame can be expressed as [21]

$$\boldsymbol{u}_s = R_s \boldsymbol{i}_s + \frac{\mathrm{d}\boldsymbol{\psi}_s}{\mathrm{d}t} \tag{1}$$

$$\boldsymbol{u}_r = R_r \boldsymbol{i}_r + \frac{\mathrm{d}\boldsymbol{\psi}_r}{\mathrm{d}t} - j\omega_r \boldsymbol{\psi}_r \tag{2}$$

$$\boldsymbol{\psi}_s = L_s \boldsymbol{i}_s + L_m \boldsymbol{i}_r \tag{3}$$

$$\boldsymbol{\psi}_r = L_m \boldsymbol{i}_s + L_r \boldsymbol{i}_r \tag{4}$$

where $\boldsymbol{u}_s$, $\boldsymbol{u}_r$, $\boldsymbol{i}_s$, $\boldsymbol{i}_r$, $\boldsymbol{\psi}_s$, and $\boldsymbol{\psi}_r$ are the stator voltage vector, rotor voltage vector, stator current vector, rotor current vector, stator flux vector, and rotor flux vector, respectively; R_s, R_r, L_s, L_r, L_m, and ω_r are the stator resistance, rotor resistance, stator inductance, rotor inductance, mutual inductance,

and electrical rotor speed, respectively.

Based on Eqs. (1)-(4), the current dynamics can be derived in the stationary frame as follows [21]

$$\frac{\mathrm{d}\boldsymbol{i}_s}{\mathrm{d}t}=-\left(\frac{R_s+\left(L_m/L_r\right)^2 R_r}{\sigma L_s}\right)\boldsymbol{i}_s+\frac{L_m}{\sigma L_s L_r}\left(\frac{1}{T_r}-j\omega_r\right)\boldsymbol{\psi}_r+\frac{1}{\sigma L_s}\boldsymbol{u}_s \tag{5}$$

$$\sigma=1-L_m^2/\left(L_s L_r\right) \tag{6}$$

3 Principle of proposed method

The proposed RPCC combines the MFC, LESO, and predictive current control. The control diagram of the proposed method is shown in Fig. 1. The details of the proposed RPCC and LESO are explained in the following sections.

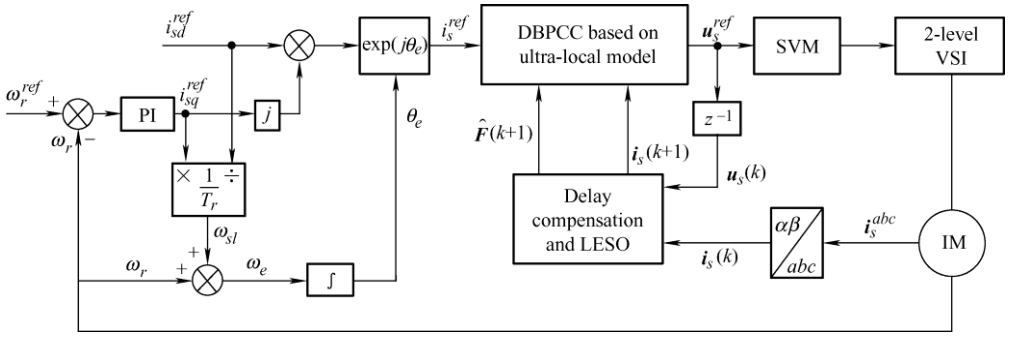

Fig. 1 Control diagram of RPCC

3.1 Ultra-local model of IM

In Ref. [20], an MFC theory that defines a single-input single-output system is proposed in the form of a first-order ultra-local model

$$\dot{y}=F+\alpha u \tag{7}$$

where u and y are the input and output variables, respectively; α is the weighting factor of the input variable; F contains uncertain parameters and disturbances. The hat ‘ · ’ denotes variable differentiation.

By comparing Eqs. (5) and (7), the stator current dynamics can be rewritten as follows

$$\begin{cases}\dfrac{\mathrm{d}\boldsymbol{i}_s}{\mathrm{d}t}=F+\alpha\boldsymbol{u}_s\\ F=-\left(\dfrac{R_s+\left(L_m/L_r\right)^2 R_r}{\sigma L_s}\right)\boldsymbol{i}_s+\dfrac{L_m}{\sigma L_s L_r}\left(\dfrac{1}{T_r}-j\omega_r\right)\boldsymbol{\psi}_r\\ \alpha=\dfrac{1}{\sigma L_s}\end{cases} \tag{8}$$

Although α contains motor parameters, the desired control performance can still be achieved by adjusting F when the motor parameters change. Thus, F should be accurately estimated to ensure satisfactory control performance.

In Ref. [22], differential algebra [23] is applied to estimate F using the input and output data over a short time. The estimated value ($\hat{F}$) can be calculated by Eq. (9) [22, 24]

$$\hat{F}=-\frac{3!}{\left(n_F T_{sc}\right)^3}\int_0^{n_F T_{sc}}\left(\left(n_F T_{sc}-2\sigma\right)\boldsymbol{i}_s\left(\sigma\right)+\alpha\sigma\left(n_F T_{sc}-\sigma\right)\boldsymbol{u}_s\left(\sigma\right)\right)\mathrm{d}\sigma \tag{9}$$

where T_{sc} is the control period, and n_F is the number of control periods. The estimation of $\hat{F}$ is relatively complicated, and the selection of n_F and T_{sc} may considerably vary in different applications [21].

3.2 Introduction of LESO

The ESO only requires a relative degree of the system [25]; hence, it can be used without the motor model.

By using the ESO to estimate the unknown part of the system in RPCC rather than using differential algebraic parameter identification techniques, the performance of RPCC has been improved, and the implementation has been simplified.

The ESO can be divided into nonlinear extended state observer (NLESO) and LESO, which has better parameter robustness [26] and simpler structure. Thus, the LESO is used in this study.

The control objects of a first-order system can be defined as [27]

$$\dot{y}=\underbrace{ay+\omega+bu}_{f}+b_0u \tag{10}$$

where y, u, and ω are the output and input variables and disturbance, respectively; a and b are unknown, and b_0 is known; f denotes the total disturbance including external and internal disturbances.

Selecting state variables $x_1=y$ and $x_2=f$, Eq. (10) can be rewritten in a state equation form

$$\begin{cases}\dot{x}_1=x_2+b_0u\\ \dot{x}_2=\dot{f}\\ y=x_1\end{cases} \tag{11}$$

According to the model-independent controller presented in Ref. [28], the corresponding continuous LESO of the system can be expressed as

$$\begin{cases}e_{rr}=z_1-y\\ \dot{z}_1=z_2+b_0u-\beta_1e_{rr}\\ \dot{z}_2=-\beta_2e_{rr}\end{cases} \tag{12}$$

where $z\to\hat{x}$, $\boldsymbol{z}$ is a state vector of the observer, and β_1 and β_2 are the gain vectors of LESO. The location of closed-loop poles of LESO can be adjusted by parameters β_1 and β_2. To ensure stability and satisfactory performance, selecting the proper β_1 and β_2 values is necessary.

From Eq. (12), the following equations can be derived

$$\begin{cases}\dot{\boldsymbol{z}}=\boldsymbol{A}\boldsymbol{z}+\boldsymbol{B}u+\boldsymbol{K}\left(y-z_1\right)\\ z_1=\boldsymbol{C}\boldsymbol{z}\end{cases} \tag{13}$$

where

$$\boldsymbol{z}=\begin{bmatrix}z_1\\ z_2\end{bmatrix}$$

$$\boldsymbol{A}=\begin{bmatrix}0 & 1\\ 0 & 0\end{bmatrix}$$

$$\boldsymbol{B}=\begin{bmatrix}b_0\\ 0\end{bmatrix}$$

$$\boldsymbol{C}=\begin{bmatrix}1 & 0\end{bmatrix}$$

$$\boldsymbol{K}=\begin{bmatrix}\beta_1\\ \beta_2\end{bmatrix}$$

Then, Eq. (13) can be rewritten as

$$\begin{cases}\dot{\boldsymbol{z}}=\left[\boldsymbol{A}-\boldsymbol{K}\boldsymbol{C}\right]\boldsymbol{z}+\left[\boldsymbol{B},\boldsymbol{K}\right]\boldsymbol{u}_0\\ y_0=\boldsymbol{z}\end{cases} \tag{14}$$

where $\boldsymbol{u}_0=\left[u,y\right]^{\mathrm{T}}$ and y_0 are the combined input and output variables, respectively.

The characteristic equation of LESO can be derived from Eq. (14) as

$$\left|s\boldsymbol{I}-\left(\boldsymbol{A}-\boldsymbol{K}\boldsymbol{C}\right)\right|=s^2+\beta_1s+\beta_2 \tag{15}$$

where $\boldsymbol{I}$ is the identity matrix.

To simplify the parameter tuning, the roots of Eq. (15) are set as $s_{1,2}=-\omega_0$ [28]. Then, Eq. (15) can be rewritten in terms of its roots as

$$s^2+\beta_1s+\beta_2=\left(s+\omega_0\right)^2 \tag{16}$$

where ω_0 is denoted as the bandwidth of the observer [28]. Solving Eq. (16), the values of β_1 and β_2 are obtained as follows

$$\begin{cases}\beta_1=2\omega_0\\ \beta_2=\omega_0^2\end{cases} \tag{17}$$

The selection of the observer bandwidth is explained in the following section.

3.3 Parameter design of LESO

Based on Eqs. (8) and (12), the LESO with the stator current as the state vector can be described as

$$\begin{cases}e_{rr}=\boldsymbol{z}_1-\boldsymbol{i}_s\\ \dot{\boldsymbol{z}}_1=\boldsymbol{z}_2+\alpha\boldsymbol{u}_s-\beta_1e_{rr}\\ \dot{\boldsymbol{z}}_2=-\beta_2e_{rr}\end{cases} \tag{18}$$

where $\boldsymbol{z}_1=\hat{\boldsymbol{i}}_s$ is the observed value of the stator current, and $\boldsymbol{z}_2=\hat{F}$ is the estimated value of disturbance F.

In digital implementation, the stator current, $\hat{\boldsymbol{i}}_s\left(k+1\right)$, and the disturbance, $\hat{F}\left(k+1\right)$, can be calculated by discretizing Eq. (18) as

$$\begin{cases}e_{rr}\left(k\right)=\hat{\boldsymbol{i}}_s\left(k\right)-\boldsymbol{i}_s\left(k\right)\\ \hat{\boldsymbol{i}}_s\left(k+1\right)=\hat{\boldsymbol{i}}_s\left(k\right)+T_{sc}\left(\hat{F}\left(k\right)+\alpha\boldsymbol{u}_s\left(k\right)\right)-\beta_{01}e_{rr}\left(k\right)\\ \hat{F}\left(k+1\right)=\hat{F}\left(k\right)-\beta_{02}e_{rr}\left(k\right)\end{cases} \tag{19}$$

where $\beta_{01}=T_{sc}\beta_1=2\omega_0T_{sc}$ and $\beta_{02}=T_{sc}\beta_2=\omega_0^2T_{sc}$ are the discrete gains of the observer.

The structural diagram of the RPCC is shown in Fig. 2.

To select the proper observer gain, assume that inductance error does not occur. The relationship between the real current and the set value can be expressed as follows

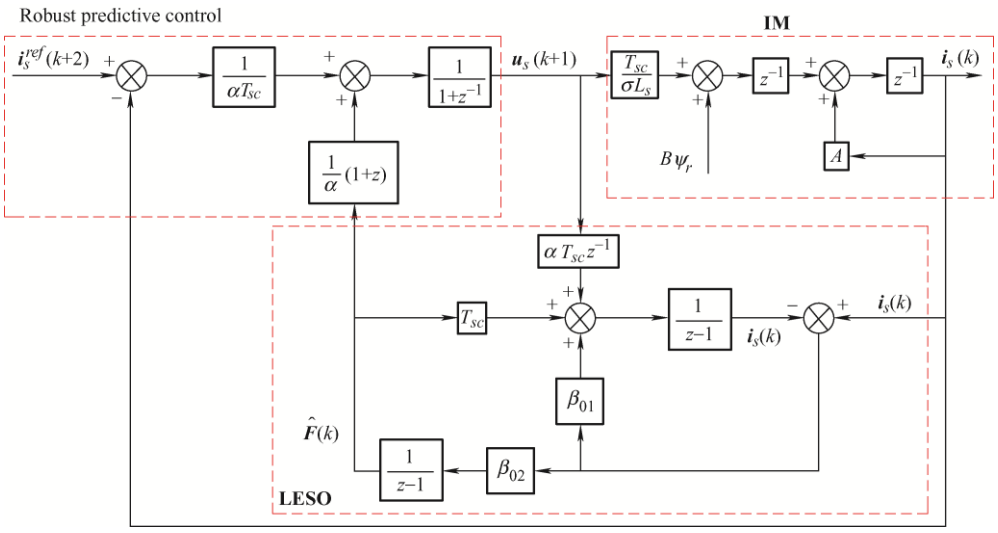

Fig. 2 Structural diagram of RPCC in z domain

$$\frac{\boldsymbol{i}_s(z)}{\boldsymbol{i}_s^{ref}(z)}=\frac{z^2+(\beta_{01}-2)z+1-\beta_{01}+\beta_{02}T_{sc}}{z^4+(\beta_{01}-2)z^3+(1+T_{sc}\beta_{02}-\beta_{01})z^2} \tag{20}$$

The characteristic equation of the system is as follows

$$z^4+(\beta_{01}-2)z^3+(1+T_{sc}\beta_{02}-\beta_{01})z^2=0 \tag{21}$$

Considering $\beta_{01}=2\omega_0 T_{sc}$ and $\beta_{02}=\omega_0^2 T_{sc}$, the roots of the characteristic equation are solved as follows

$$z_{1,2}=0 \tag{22}$$

$$z_{3,4}=1-\omega_0 T_{sc} \tag{23}$$

Then, ω_0 can be computed from Eq. (23) as follows

$$\omega_0=\frac{1-z_{3,4}}{T_{sc}} \tag{24}$$

To ensure stability, ω_0 should be selected to satisfy $|z_{3,4}|<1$. Generally, when ω_0 is extremely small ($z_{3,4}$ approaches 1), the dynamic performance is inadequate. When ω_0 is extremely large ($z_{3,4}$ approaches -1), the robustness of the system is decreased [29]. In this work, $z_{3,4}$ is set to 0.5, and the corresponding ω_0 is 5 000 when the sampling frequency is 10 kHz.

3.4 Prediction of current and voltage

Combining Eqs. (8) and (19), the stator voltage vector at the kth instant can be derived as follows

$$\boldsymbol{u}_s(k)=-\frac{\hat{F}(k)}{\alpha}+\frac{\boldsymbol{i}_s^{ref}(k+1)-\boldsymbol{i}_s(k)}{\alpha T_{sc}} \tag{25}$$

However, there is usually a one-step delay in the digital control system [4]. To compensate for the influence of digital delay, the stator voltage vector reference has to be calculated using Eq. (26)

$$\boldsymbol{u}_s^{ref}=-\frac{\hat{F}(k+1)}{\alpha}+\frac{\boldsymbol{i}_s^{ref}(k+2)-\boldsymbol{i}_s(k+1)}{\alpha T_{sc}} \tag{26}$$

where $\boldsymbol{i}_s(k+1)$ can also be obtained by the LESO according to Eq. (19).

$$\boldsymbol{i}_s(k+1)=\boldsymbol{i}_s(k)+T_{sc}\left(\hat{F}(k)+\alpha\boldsymbol{u}_s(k)\right) \tag{27}$$

The reference stator current vector in the stationary frame at the (k+2)th instant can be expressed as

$$\boldsymbol{i}_s^{ref}(k+2)=(i_{sd}^{ref}+ji_{sq}^{ref})\exp(j\theta_e^{k+2}) \tag{28}$$

$$\theta_e^{k+2}=\theta_e^k+2\omega_e^k T_{sc} \tag{29}$$

where θ_e^k is the position of the rotor flux linkage vector at the kth instant, and ω_e^k is the rotational speed of the rotor flux linkage vector.

4 Experimental results

To verify the advantages of the proposed RPCC, it is compared with the deadbeat predictive current control (DBPCC) and conventional MFPCC on a two-level inverter-fed IM drive platform. The conventional MFPCC represents an MFPCC that uses differential algebra (Eq. (9)) to estimate the ultra-local model; Fig. 3 shows the experimental setup. The machine and observer parameters applied to the test are listed in Tab. 1. The control algorithm is implemented on a 32-bit floating DSP TMS320F28335, and the sampling frequency is 10 kHz. In the

experimental results, the stator current is sampled by a current probe. The motor speed and q-axis and d-axis currents are obtained via an on-board digital-to-analog converter. All data are acquired by a scopecorder (YOKOGAWA DL850) and plotted on a personal computer using Matlab.

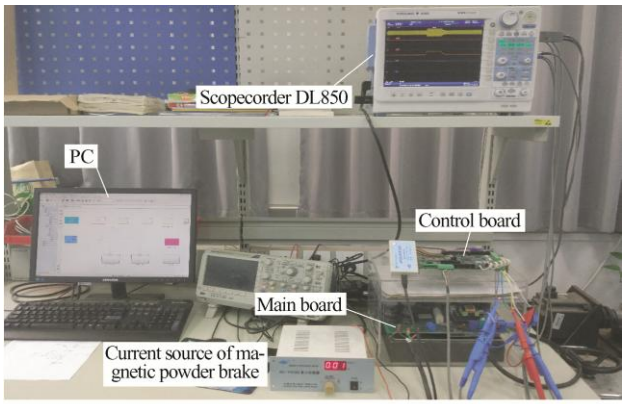

(a) Inverter and oscilloscope

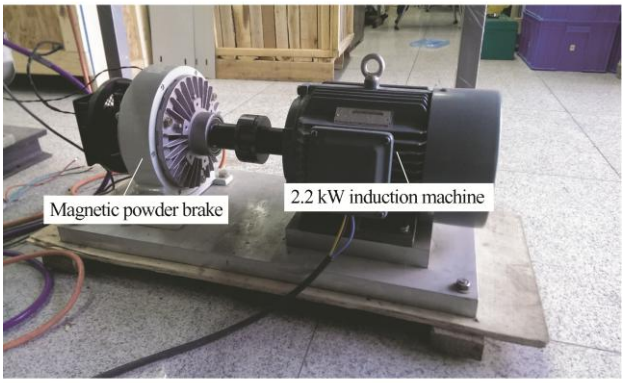

(b) 2.2 kW IM and magnetic powder brake

Fig. 3 Experimental setup of two-level inverter-fed IM drive

Tab. 1 Machine and control parameters

Parameter	Value
DC-bus voltage U_{dc}/V	540
Rated power P_N/kW	2.2
Rated voltage U_N/V	380
Rated frequency f_N/Hz	50
Rated torque T_N/(N·m)	14
Number of pole pairs N_p	2
Stator resistance R_S/Ω	3.065
Rotor resistance R_r/Ω	1.879
Mutual inductance L_m/H	0.232
Stator inductance L_s/H	0.242
Rotor inductance L_r/H	0.242
Flux amplitude reference φ_s/Wb	0.85
Control period T_{SC}/μs	100
Observer parameter α	50.5
Observer parameter ω_0	5 000

4.1 Dynamic performance

The performance during the transient process is tested for the DBPCC, conventional MFPCC, and proposed RPCC. The results when the motor starts from standstill to 1 500 r/min with no load and with inaccurate parameters set in the controller are shown in Figs. 4 and 5. From top to bottom, the curves in these figures represent the motor speed, q-axis current (i_q), d-axis current (i_d), and one-phase stator current (i_a).

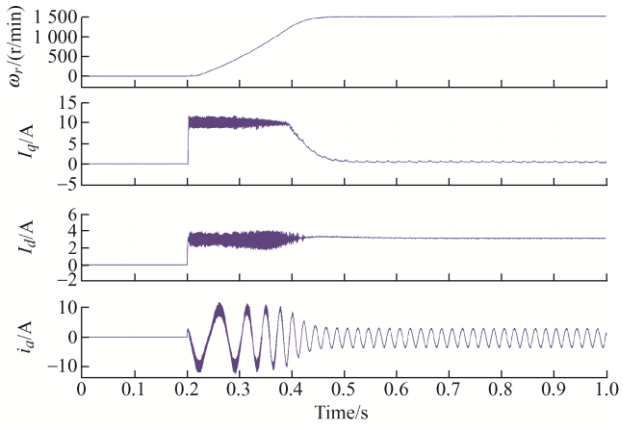

(a) DBPCC

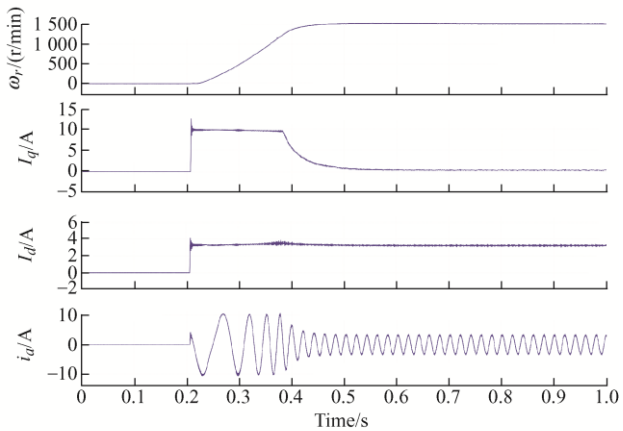

(b) Conventional MFPCC

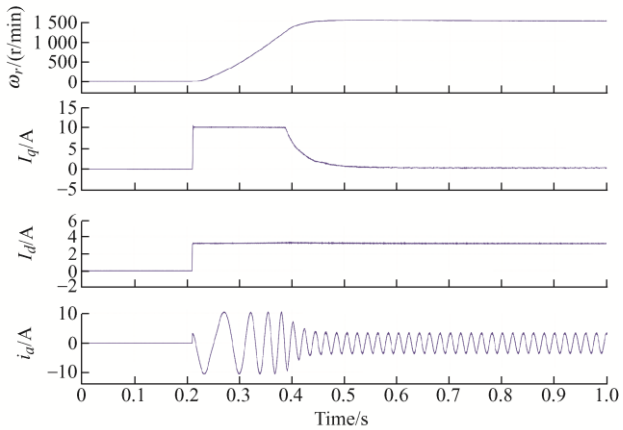

(c) Proposed RPCC

Fig. 4 Starting response from standstill to rated speed when all parameters increase to three times normal values

The responses when all parameters (stator resistance R_s, rotor resistance R_r, stator inductance L_s, rotor inductance L_r, and mutual inductance L_m) used in the controller become three times their normal values

are shown in Fig. 4. The results when all parameters are half of their nominal values are presented in Fig. 5. For the DBPCC, significant current ripples or tracking errors are observed when the parameters are not accurate. As shown in Figs. 4b and 5b, although the conventional MFPCC can achieve a fast starting response when the motor parameters are not accurate, some ripples are observed in the *dq*-axis current during motor acceleration. The dynamic responses of the proposed RPCC with different parameter mismatches are shown in Figs. 4c and 5c. The figures clearly show that the proposed RPCC can achieve the best performance without the influence of parameter mismatches.

4.2 Steady-state response

The steady-state responses of the DBPCC, conventional MFPCC, and proposed RPCC with accurate motor parameters are shown in Fig. 6. Based on the figure, all methods can achieve a stable operation. However, the conventional MFPCC exhibits slightly larger current

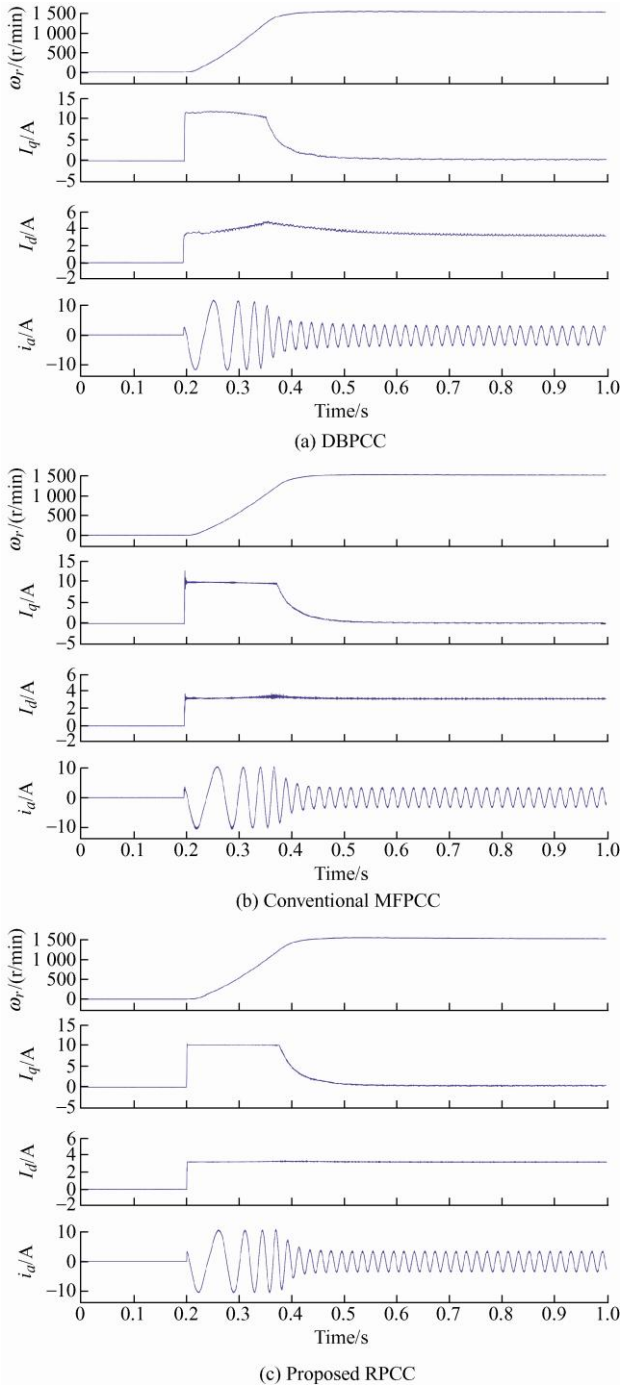

Fig. 5 Starting response from standstill to the rated speed when all parameters become half of normal values

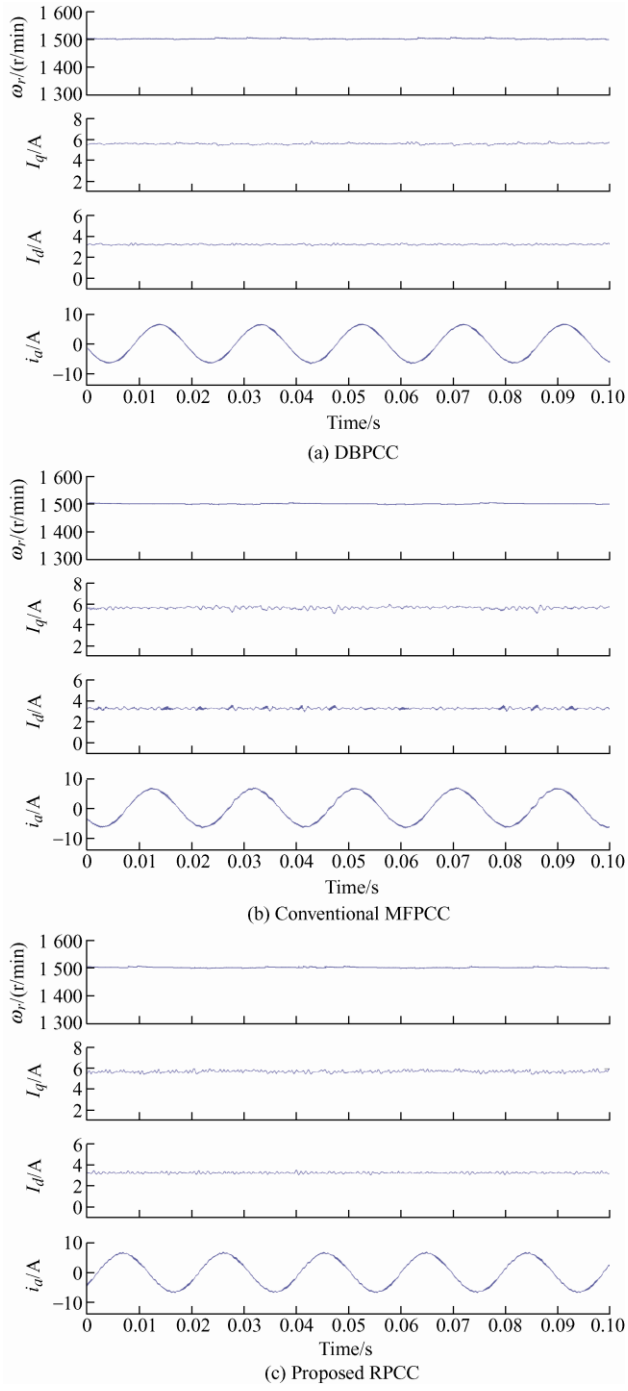

Fig. 6 Responses at 1 500 r/min with rated load and accurate parameters

ripples. The total harmonic distortions (THDs) of the current at different speeds with the rated load are shown in Fig. 7. The steady-state performance of the proposed RPCC is comparable with that of the DBPCC when the model parameters are accurate. The RPCC clearly has a lower stator current THD than the conventional MFPCC at all testing points.

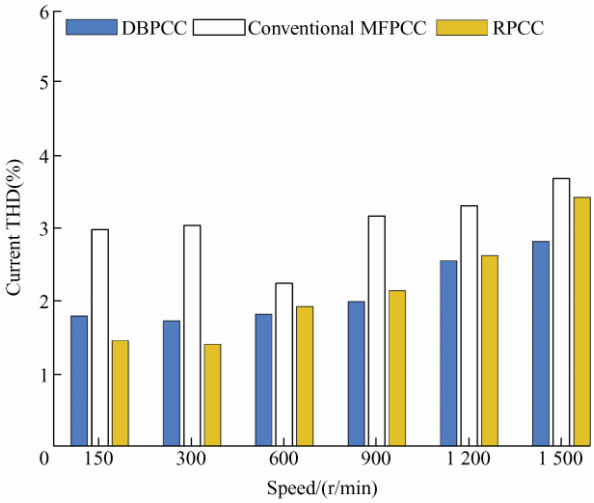

Fig. 7 THD of stator current at different speeds without parameter mismatches for DBPCC, conventional MFPCC and the proposed RPCC

Performance comparisons with parameter errors are also conducted. The steady-state responses of the DBPCC, conventional MFPCC, and proposed RPCC with inaccurate motor parameters are shown in Figs. 8-11. In these figures, *All*=*n* pu denotes that all model parameters used in the control algorithm are *n* times their actual values. A similar description is applied to resistance (R_s and R_r) and inductance (L_s, L_r, and L_m).

The results at 150 r/min under the rated load with smaller estimated motor parameters for the DBPCC are shown in Fig. 8a. The results show that the performance under low-speed operation is not significantly affected when the motor parameters set in the control algorithm are smaller.

The results at 150 r/min under the rated load with larger estimated motor parameters for the DBPCC are shown in Fig. 9a. Larger stator resistance results are observed in certain deviations of the *dq*-axis current. If the rotor resistance is large, the DBPCC can still achieve satisfactory control performance. However, if the inductance is large, significant ripples in the *dq*-axis current are observed. From the foregoing tests, the DBPCC is found to be sensitive to overestimated inductance at a low-speed operation.

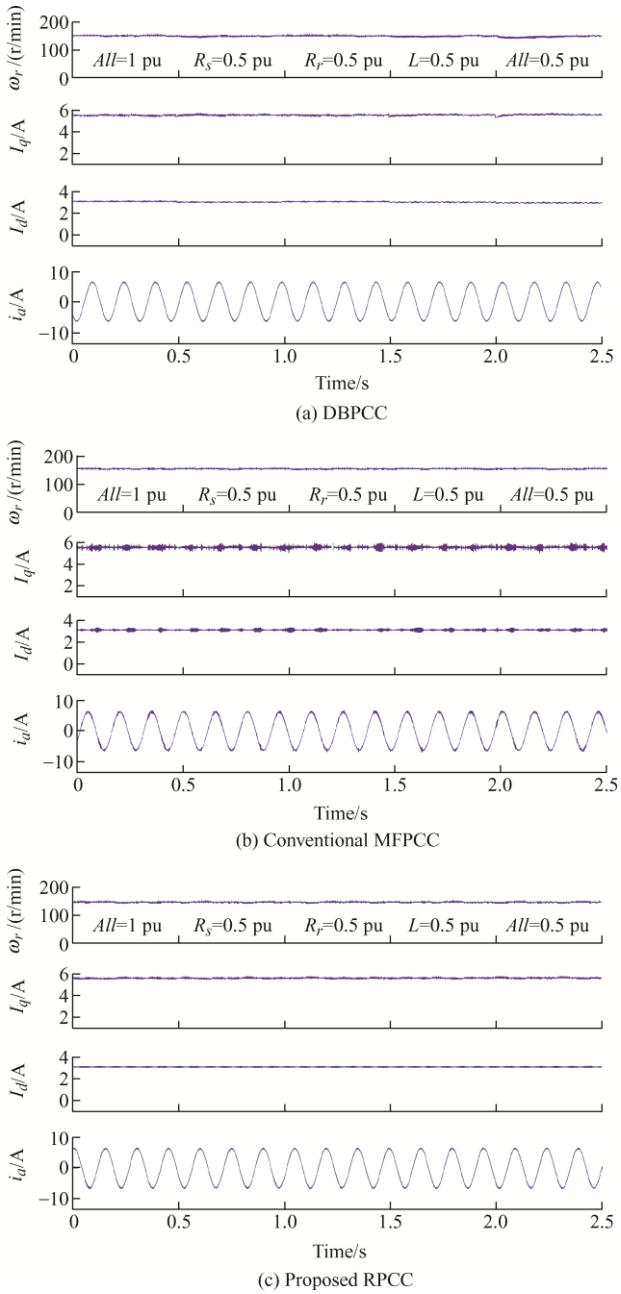

Fig. 8 Responses at 150 r/min with rated load with smaller parameters

In contrast, Figs. 8b and 9b indicate that the conventional MFPCC can achieve stable operation

with different motor parameter errors.

The results for the proposed RPCC are shown in Figs. 8c and 9c. Compared with the differential algebra method, the LESO can more accurately estimate $\boldsymbol{F}$; hence, the proposed RPCC can achieve a better steady-state performance.

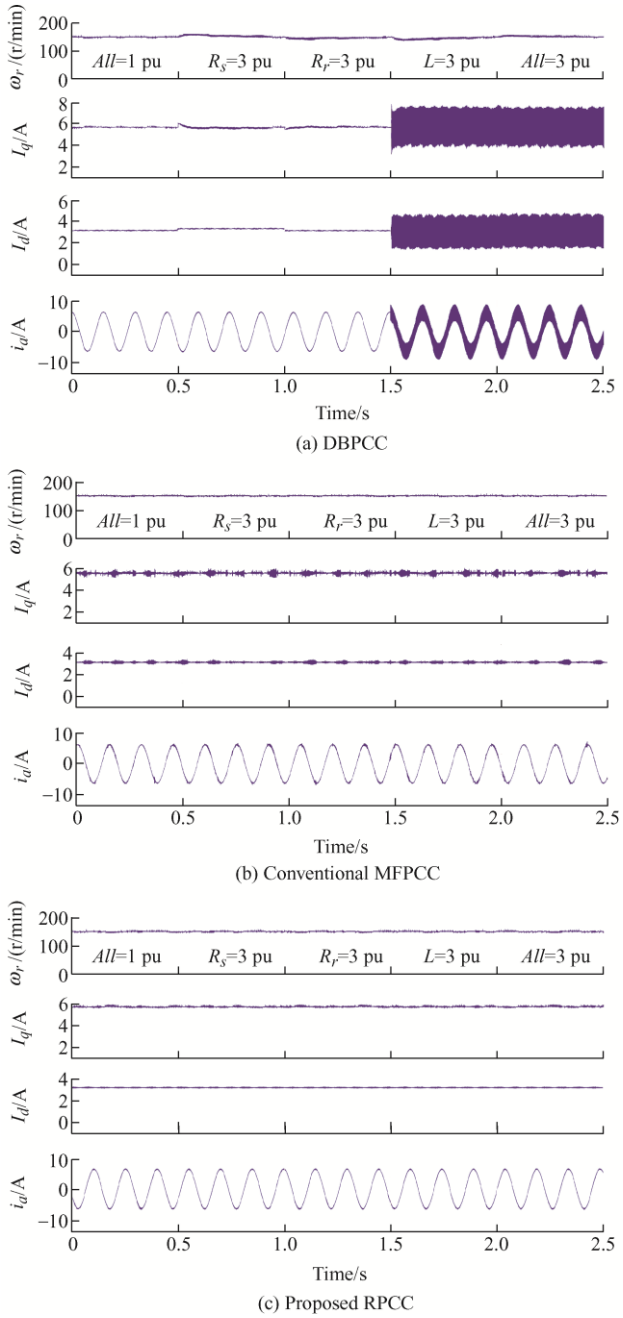

(a) DBPCC

(b) Conventional MFPCC

(c) Proposed RPCC

Fig. 9 Responses at 150 r/min with rated load with larger parameters

The results at 1 500 r/min under the rated load for the DBPCC are illustrated in Figs. 10a and 11a. If the inductance is less than the accurate value, the system finally loses stability. If the inductance is larger than the accurate value, distinct stator current harmonics are observed.

The results at 1 500 r/min under the rated load for the conventional MFPCC are shown in Figs. 10b and 11b. The conventional MFPCC exhibits acceptable parameter robustness, and satisfactory performance can still be achieved despite parameter mismatches.

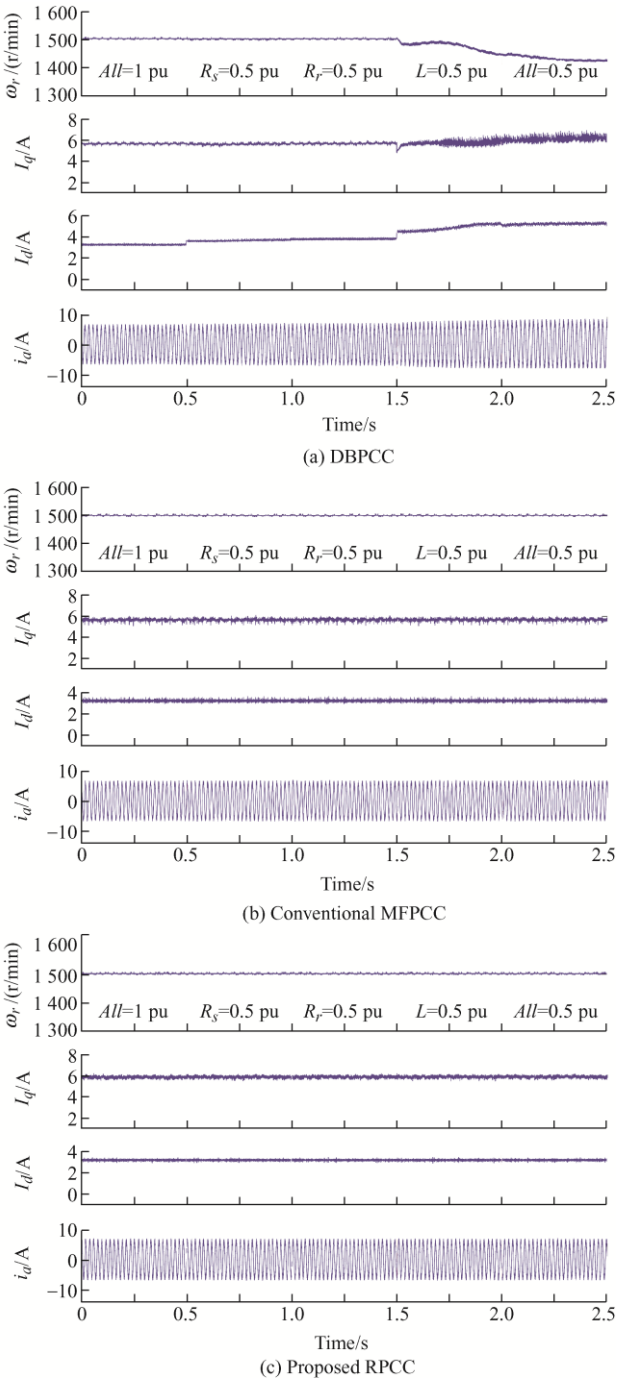

(a) DBPCC

(b) Conventional MFPCC

(c) Proposed RPCC

Fig. 10 Responses at 1 500 r/min with rated torque and smaller parameters

The results shown in Figs. 10c and 11c are consistent with those shown in Figs. 8c and 9c. The proposed RPCC can achieve better steady-state

performance under parameter mismatches.

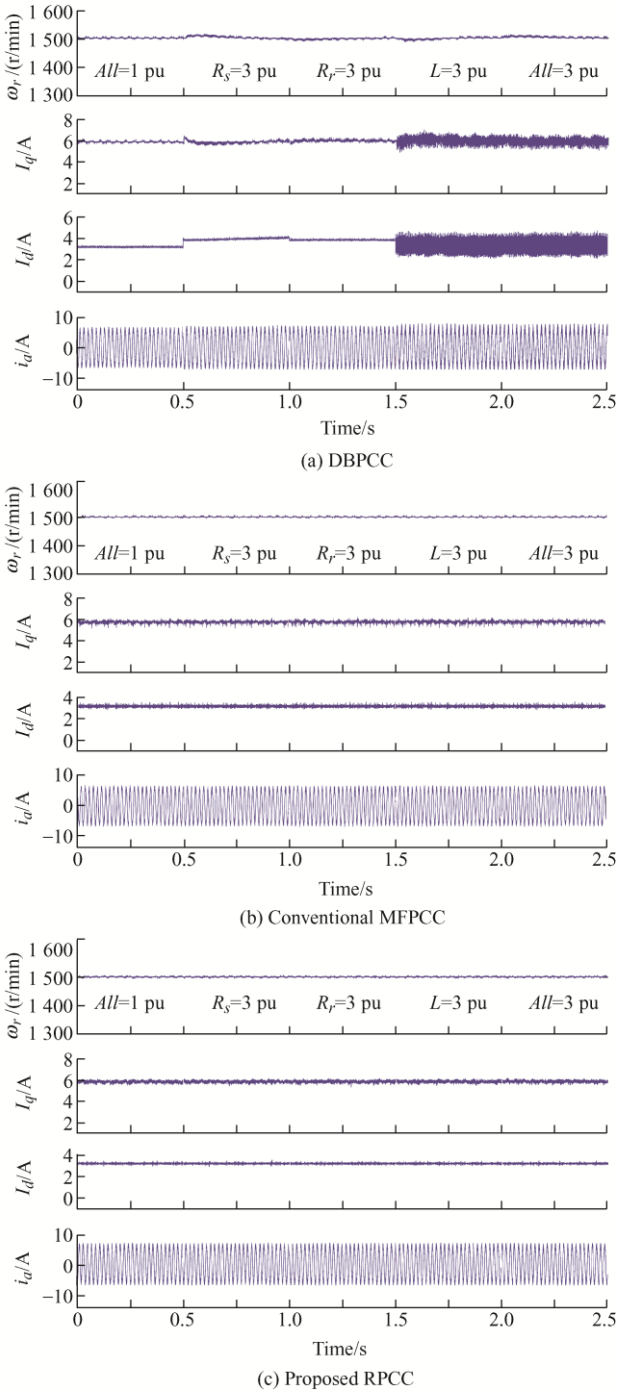

Fig. 11 Responses at 1 500 r/min with rated torque with larger parameters

5 Conclusions

In practical implementation, motor parameters may change under different working conditions and environments. The conventional predictive current control is sensitive against parameter mismatches because many motor parameters are used in the algorithm. If large parameter errors exist, both the dynamic and steady-state performance levels deteriorate. To resolve this problem, the RPCC method for IM drives based on the ultra-local model and LESO is proposed in this paper. Compared with the DBPCC, the proposed method uses the input and output data of the system without requiring an accurate system model. Hence, it is robust against the estimation errors of motor parameters. The experimental results validate that the proposed RPCC achieves satisfactory control performance over a wide speed range even with parameter mismatches.

References

[1] H A Zarchi, H M Hesar, M A Khoshhava. Online maximum torque per power losses strategy for indirect rotor flux-oriented control-based induction motor drives. *IET Electr. Power Appl.*, 2019, 13(2): 259-265.

[2] D Casadei, G Serra, A Tani, et al. Performance analysis of a speed-sensorless induction motor drive based on a constant switching-frequency DTC scheme. *IEEE Trans. Ind. Appl.*, 2003, 39(2): 476-484.

[3] D Casadei, F Profumo, G Serra, et al. FOC and DTC: Two viable schemes for induction motors torque control. *IEEE Trans. Power Electron*., 2002, 17(5): 779-787.

[4] J Rodriguez, M P Kazmierkowski, J R Espinoza, et al. State of the art of finite control set model predictive control in power electronics. *IEEE Trans. Ind. Inf.*, 2013, 9(2): 1003-1016.

[5] Y Zhang, B Xia, H Yang, et al. Overview of model predictive control for induction motor drives. *Chinese Journal of Electrical Engineering*, 2016, 2(1): 62-76.

[6] S Vazquez, J Rodriguez, M Rivera, et al. Model predictive control for power converters and drives: Advances and trends. *IEEE Trans. Ind. Electron*., 2017, 64(2): 935-947.

[7] H Miranda, P Cortes, J Yuz, et al. Predictive torque control of induction machines based on state-space models. *IEEE Trans. Ind. Electron*., 2009, 56(6): 1916-1924.

[8] Y Zhang, H Yang, B Xia. Model-predictive control of induction motor drives: Torque control versus flux control. *IEEE Trans. Ind. Appl.*, 2016, 52(5): 4050-4060.

[9] S A Davari, D A Khaburi, R Kennel. An improved FCS-MPC algorithm for an induction motor with an imposed optimized weighting factor. *IEEE Trans. Power Electron*., 2012, 27(3): 1540-1551.

[10] I J Ha, S H Lee. An online identification method for both

stator-and rotor resistances of induction motors without rotational transducers. *IEEE Trans. Ind. Electron.*, 2000, 47(4): 842-853.

[11] P N Phuc, H Vansompel, D Bozalakov, et al. Data-driven online temperature compensation for robust fieldoriented torque-controlled induction machines. *IET Electr. Power Appl.*, 2019, 13(2): 1954-1963.

[12] H Yang, Y Zhang, J Liang, et al. Robust deadbeat predictive power control with a discrete-time disturbance observer for PWM rectifier under unbalanced grid conditions. *IEEE Trans. Power Electron.*, 2019, 34(1): 287-300.

[13] J Wang, F Wang, Z Zhang, et al. Design and implementation of disturbance compensation-based enhanced robust finite control set predictive torque control for induction motor systems. *IEEE Trans. Ind. Inf.*, 2017, 13(5): 2645-2656.

[14] Y Zhou, H Li, H Yao. Model-free control of surface mounted PMSM drive system. *International Conference on Industrial Technology (ICIT)*, 2016, Taipei, Taiwan, China. IEEE, 2016: 175-180.

[15] D Q Dang, M S Rafaq, H H Choi, et al. Online parameter estimation technique for adaptive control applications of interior pm synchronous motor drives. *IEEE Trans. Ind. Electron.*, 2016, 63(3): 1438-1449.

[16] T Boileau, N Leboeuf, B N Mobarakeh, et al. Online identification of PMSM parameters: Parameter identifiability and estimator comparative study. *IEEE Trans. Ind. Appl.*, 2011, 47(4): 1944-1957.

[17] Z Yin, Y Zhang, C Du, et al. Research on anti-error performance of speed and flux estimation for induction motors based on robust adaptive state observer. *IEEE Trans. Ind. Electron.*, 2016, 63(6): 3499-3510.

[18] S Chang, P Chen, Y Ting, et al. Robust current control-based sliding mode control with simple uncertainties estimation in permanent magnet synchronous motor drive systems. *IET Electr. Power Appl.*, 2010, 4(6): 441-450.

[19] C Lin, T Liu, J Yu, et al. Model-free predictive current control for interior permanent-magnet synchronous motor drives based on current difference detection technique. *IEEE Trans. Ind. Electron.*, 2014, 61(2): 667-681.

[20] M Fliess, C Join. Model-free control and intelligent PID controllers: Towards a possible trivialization of nonlinear control. *IFAC Proceedings Volumes*, 2009, 42(10): 1531-1550.

[21] R Bojoi, E Levi, F Farina, et al. Dual three phase induction motor drive with digital current control in the stationary reference frame. *IEE Proceedings-Electric Power Applications*, 2006, 153(1): 129-139.

[22] M Fliess, C Join. Model-free control. *Int. J. Control*, 2013, 86(12): 2228-2252.

[23] M Mboup, C Join, M Fliess. Numerical differentiation with annihilators in noisy environment. *Numerical Algorithms*, 2009, 50(4): 439-467.

[24] L L Cao, H M Li, H G Zhang. Model-free power control of front-end PFC AC/DC converter for on-board charger. *International Power Electronics and Motion Control Conference (IPEMC-ECCE Asia)*, 2016, Hefei, China. IEEE, 2016: 2719-2723.

[25] A J Humaidi, H M Badr, A R Ajil. Design of active disturbance rejection control for single-link flexible joint robot manipulator. *International Conference on System Theory, Control and Computing (ICSTCC)*, 2018, Sinaia. IEEE, 2018: 452-457.

[26] A J Humaidi, I K Ibraheem. Speed control of permanent magnet DC motor with friction and measurement noise using novel nonlinear extended state observer-based anti-disturbance control. *Energies*, 2019, 12(9): 1651.

[27] A Safaei, M N Mahyuddin. Adaptive model-free control based on an ultra-local model with model-free parameter estimations for a generic siso system. *IEEE Access*, 2018, 6: 4266-4275.

[28] Z Q Gao. Scaling and bandwidth-parameterization based controller tuning. *Proceedings of the 2003 American Control Conference*, 2003, Denver, CO, USA. IEEE, 2003: 4989-4996.

[29] Q Xu, M Sun, Z Chen, et al. Analysis and design of the extended state observer using internal mode control. *Proceedings of the 32nd Chinese Control Conference*, 2013, Xi'an, China. IEEE, 2013: 5408-5413.

Yongchang Zhang (M'10-SM'18) received his B.S. degree from Chongqing University, China, in 2004 and his Ph.D. degree from Tsinghua University, China, in 2009; both degrees are in electrical engineering.

From August 2009 to August 2011, he was a postdoctoral fellow at the University of Technology Sydney, Australia. He joined North China University of Technology in August 2011 as an associate professor and then a full professor since 2015. Currently he is a full professor with North China Electric Power University, Beijing, China. He has published more than 100 technical papers in the area of motor drives, pulse width modulation and AC/DC converters. His current research interest is model predictive control for power converters and motor drives.

Xing Wang was born in 1997. He received his B.S. degree in electrical engineering in 2018 from the North China University of Technology, Beijing, China, where he is currently working toward his M.S. degree in control science and engineering. His research interests include model predictive control of induction motor drives.

Haitao Yang received his B.S. degree from the Hefei University of Technology, Hefei, China, in 2009 and his M.S. degree from the North China University of Technology, Beijing, China, in 2015; both degrees are in electrical engineering. He is presently working toward his Ph.D. degree with the University of Technology Sydney, Ultimo, NSW, Australia. He is currently with the North China University of Technology, Beijing, China. His research interests include control of motor drives, PWM converters, and electric vehicles.

Boyue Zhang was born in 1993. He received his B.S. degree in electrical engineering and automation from Liaoning Technical University, Liaoning, China, in 2017. He is currently working toward his master's degree in electrical engineering at the North China University of Technology, Beijing, China. His research interests include the MPC of IM drives.

Jose Rodriguez (Life Fellow, IEEE) received his degree in electrical engineering from Universidad Tecnica Federico Santa Maria, Valparaiso, Chile, in 1977 and his Dr.Eng degree in electrical engineering from the University of Erlangen, Erlangen, Germany, in 1985. He has been with the Department of Electronics Engineering, Universidad Tecnica Federico Santa Maria since 1977 as a full professor and became president of this university in 2015. Since 2019, he has been a full professor with Universidad Andres Bello, Santiago, Chile. He has coauthored two books, several book chapters, and more than 400 journal and conference articles. His main research interests include multilevel inverters, new converter topologies, control of power converters, and adjustable-speed drives. He has received a number of best paper awards from IEEE journals.

He is a member of the Chilean Academy of Engineering. He was a recipient of the National Award of Applied Sciences and Technology from the government of Chile in 2014, and the Eugene Mittelmann Award from the Industrial Electronics Society of the IEEE in 2015.